Skeletal Radiol (2007) 36:229–235
DOI 10.1007/s00256-006-0211-4

TECHNICAL REPORT

Calculation of rotational deformity in pediatric supracondylar humerus fractures

Eric R. Henderson · Kenneth A. Egol · Harold J. P. van Bosse · Mark E. Schweitzer · Sarah K. Pettrone · David S. Feldman

Received: 27 July 2006 / Revised: 17 August 2006 / Accepted: 23 August 2006 / Published online: 1 December 2006

Abstract
Objective Supracondylar humerus fractures (SCHF) are common in the pediatric population. Cubitus varus deformity (CVD) is the most common long-term complication of SCHFs and may lead to elbow instability and deficits in throwing or extension. Distal fragment malrotation in the axial plane disposes to fragment tilt and CVD; however, no simple method of assessing fracture malrotation exists. This study tested a mathematical method of measuring axial plane malrotation in SCHFs based on plain radiographs.
Design A pediatric SCHF model was made, and x-rays were taken at known intervals of rotation. Five independent, blinded observers measured these films. Calculated rotation for each data set was compared to the known rotation. The identical protocol was performed for an aluminum phantom.
Results The reliability and agreement of the rotation values were good for both models.
Conclusions This method is a reliable, accurate, and cost-effective means of calculating SCHF distal fragment malrotation and warrants clinical application.

This study was conducted at the NYU Hospital for Joint Diseases. None of the authors received financial support for this study.

E. R. Henderson · K. A. Egol · H. J. P. van Bosse · M. E. Schweitzer · S. K. Pettrone · D. S. Feldman
NYU Hospital for Joint Diseases,
301 East 17th Street,
New York, NY 10003, USA

D. S. Feldman (✉)
Pediatric Orthopaedic Surgery, Center for Children,
NYU Hospital for Joint Diseases,
301 East 17th Street,
New York, NY 10003, USA
e-mail: david.feldman@med.nyu.edu

Keywords Supracondylar fracture · Humeral fracture · Humerus · Rotation · Radiograph · Mathematical model

Introduction

Fractures about the elbow account for 5–10% of all fractures in children; 50–70% of these are supracondylar humerus fractures (SCHFs) [1]. These occur most commonly in males at a mean age of 6.7 years (range 3–10). The majority of these fractures are caused by falls and usually affect the nondominant arm [2]. Physiological hyperextension of the elbow is common in the affected age group. When a sufficient load is applied to the hyperextended elbow and transmitted through the olecranon to the thin bone of the olecranon fossa, an extension-type SCHF results [1, 3–8].

SCHFs may present an immediate risk of neurovascular damage. Treatment is technically demanding due to the complex anatomy and the significant risk of deformity [1–3, 9–13]. Current management for displaced fractures consists of closed reduction and percutaneous pinning when possible. If closed reduction is unsuccessful then open reduction is performed. Despite this standardized treatment, cubitus varus deformity (CVD) is the most common long-term complication of SCHF (Fig. 1) [14–21]. The primary etiology of CVD is tilting of the distal fragment in the coronal plane [16]. Malrotation of the distal fragment in the axial plane disposes to fragment tilt leading to CVD [14, 18, 22–24]. Short-term disability with CVD is seen occasionally in throwing athletes and with extension activities such as push ups or bench pressing; however, the immediate effects are mainly cosmetic [25]. Long-term follow-up of patients with CVD secondary to pediatric SCHF shows that medial displacement of the humerus's

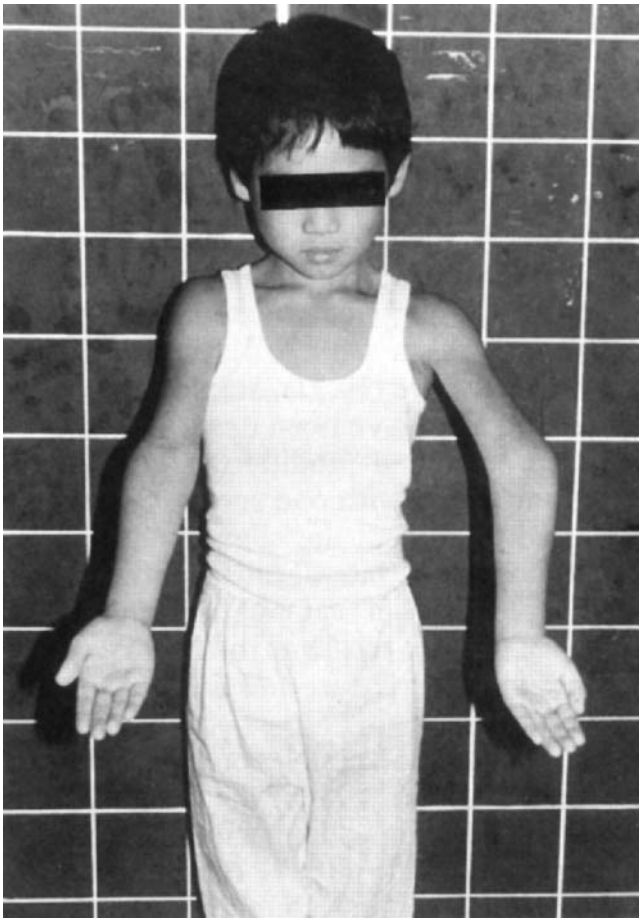

Fig. 1 Cubitus varus deformity in a pediatric patient (from Uchida Y, Ogtata K, Sugioka Y. A new three-dimensional osteotomy for cubitus varus deformity after supracondylar fracture of the humerus in children. J Ped Orthop 1991;11:327–331)

Fig. 2 Pediatric supracondylar humerus fracture model mounted in wood frame

mechanical axis and the triceps line of pull cause stretching of the lateral collateral ligament complex producing posterolateral rotatory instability of the elbow joint [26].

Because rotational malalignment does not remodel, it is suggested that up to 30–45° of axial plane rotation can be accepted in the final reduction as rotation at the shoulder can compensate for moderate rotational deformity at the distal humerus [7]. Despite these recommendations, no simple method of assessing the degree of fracture malrotation exists in the literature. The purpose of this study was to test a mathematical method of measuring axial plane malrotation in SCHFs.

Materials and methods

We developed a method of calculating SCHF fragment rotation using measurements from anteroposterior (AP) and lateral radiographs. We used a radioopaque left pediatric humerus model (Sawbones, Vashon, WA) to create a transverse SCHF model (Fig. 2). The proximal end was osteotomized in the axial plane through the center of the humeral head to provide a flat surface for mounting a goniometer (Perrygraf, Carol Stream, IL). A rigid, wooden frame was constructed with 1-in thick plywood. The distal fragment was secured to the frame with two metal pins and epoxy. Another metal rod was then inserted through the length of the proximal and distal Sawbones pieces and functioned as the axis of rotation.

A control phantom with smooth, symmetrical contours was created to confirm the validity of the mathematical model and allow comparison of the asymmetric humerus model with an object that would generate a predictable image as it rotated (Fig. 3). For this model an oblong aluminum block with rounded lateral edges was cut in half to produce two identical pieces. These were threaded over a steel rod with a goniometer mounted between them. Epoxy was used to affix each arm of the goniometer to its adjacent aluminum piece. The rod was mounted in a wooden frame.

Digitized AP and lateral radiographs of the model humerus were obtained (Fig. 4). Radiographs were taken of the humerus in 5° increments of rotation ranging from 0° to 90° of external rotation of the proximal fragment. External rotation of the proximal fragment was simulated as elbow

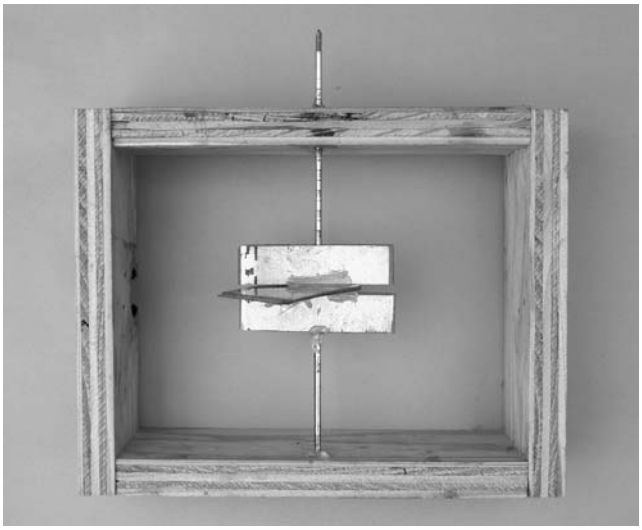

Fig. 3 Aluminum phantom model mounted in wood frame

radiographs are commonly oriented with respect to the forearm and thus internal rotation of the distal fracture fragment is seen as external rotation of the proximal bone on radiographs. An identical procedure was followed for the aluminum phantom radiographs (Fig. 5).

Two pediatric orthopaedic surgeons, an orthopaedic traumatologist, a musculoskeletal radiologist, and a senior orthopaedic resident independently measured the radiographs on a Siemens Magicview VE 42 PACS MV1000 monitor. The observers were blinded to the protocol used to take the radiographs. On each AP film the dimensions of the distal fracture line and the proximal fracture line were measured (Fig. 6). On the lateral view the distal fracture-line dimension was measured (Fig. 6). These measurements were made with electronic calipers to the hundredth of a centimeter on magnified images. Observers were allowed to modify the image to their liking prior to making each measurement. The values of each observer were recorded in a spreadsheet (Microsoft Excel, Redmond, WA). Radiographs of the aluminum phantom were measured in the same manner.

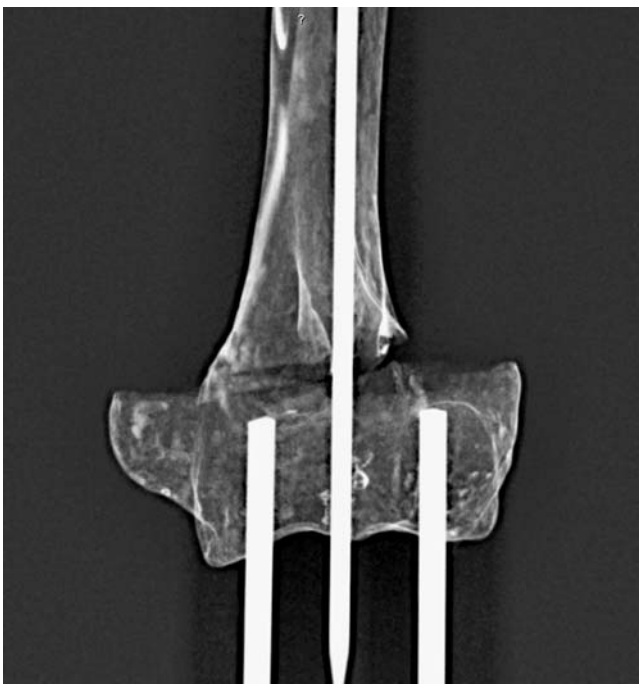

Fig. 4 AP radiograph of humerus model at 60° rotation

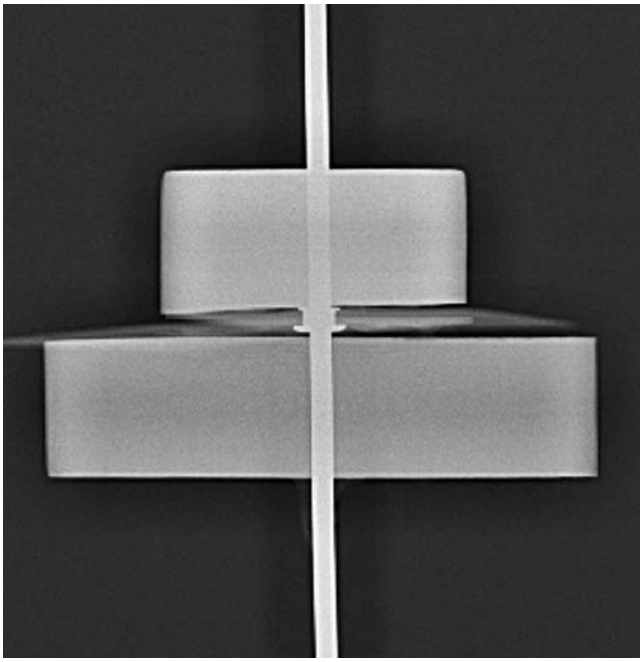

Fig. 5 AP radiograph of aluminum phantom model at 60° rotation

Our method of calculating distal fracture-fragment rotation from these radiographic measurements is based upon the oblong cross-sectional shape of the distal humerus. When in anatomic position, the AP dimension

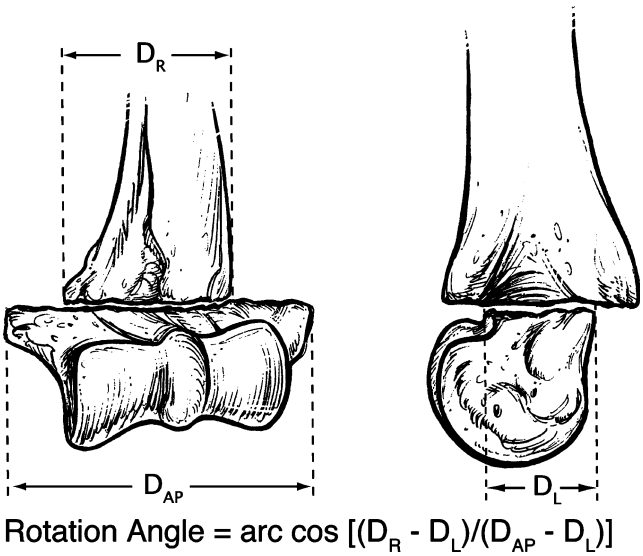

Fig. 6 AP and lateral illustrations of supracondylar humerus fracture with measurements and equation for rotation calculation

of the distal humerus is three to four times greater than its lateral dimension, see D_{AP} and D_L (Fig. 6). Therefore rotation of either the proximal or distal fracture fragment in the axial plane, as seen with unstable reduction, will cause the dimensions of the images seen on AP and lateral radiographs to vary as the fragment turns.

The equation in Fig. 6 is used to calculate the fracture-fragment rotation. Derivation of this equation is based on the close resemblance that a cross section of the distal humerus bears to an ellipse. An ellipse is a rounded shape whose major and minor dimensions, which for simplicity we name D_{AP} and D_L, respectively, are perpendicular (Fig. 7). The total change in these dimensions that occurs if the fragment rotates 90° is the difference between the AP and lateral dimensions of the bone at the site of the fracture, in other words $D_{AP}-D_L$. If the ellipse were very thin, i.e., $D_L=0$, then the measured width of the rotating ellipse, D_R, viewed from the standpoint where the starting dimension is D_{AP}, would be defined by:

$$D_R = D_{AP} * \text{cosine}\,\theta \quad (1)$$

As with the ellipse in Fig. 7, however, the distal humerus has a D_L value that is greater than zero and this must be taken into account. Because the measurement of D_R can vary by the amount $D_{AP}-D_L$, this amount is now multiplied by cosine and added to D_L in order to calculate D_R:

$$D_R = [\text{cosine}\,\theta(D_{AP} - D_L)] + D_L \quad (2)$$

Now the ellipse will measure D_{AP} when no rotation has occurred and D_L when it has rotated 90°. Because D_L, D_R, and D_{AP} are measurable on x-ray (see Fig. 6), and we wish to know the angle of rotation, θ, the equation is rearranged:

$$\theta = \text{arc cosine}[(D_R - D_L)/(D_{AP} - D_L)] \quad (3)$$

The angle of rotation can now be calculated with the three measurements performed by the observers: D_L, D_R, and D_{AP} (Fig. 6).

Statistical analysis was done with the Statistical Package for Social Sciences 10.0 (Chicago, IL). Interobserver reliability was quantified by calculating the intraclass correlation coefficients (2,1) [ICC (2,1)] [27] for results from the model humerus and aluminum phantom. Agreement between the calculated rotation and the actual rotation within 3° and 5° was calculated and reported as a percentage.

To better facilitate use of this method in the clinical setting, where a calculator is not always available, a list of approximate ratios corresponding to angles of fragment rotation is available in Table 1. The arithmetic to calculate the ratio would be taken from Eq. 3:

$$\text{ratio} = [(D_R - D_L)/(D_{AP} - D_L)] \quad (4)$$

Results

Calculated rotation values for the model humerus and the aluminum phantom were close to the actual rotation values throughout the 90° arc of rotation with better agreement for the aluminum model. Plots of the rotation values calculated from the measurements of the five observers are seen in Figs. 8 and 9. As seen in Fig. 8, accuracy of the calculated rotation for the model humerus varied uniformly for all observers through the 90° arc of rotation. This variation was not seen with the aluminum phantom and was therefore attributed to humerus asymmetry. Because of this variance, percent agreement of the calculated rotation to the actual rotation was reported in increments of 10°, see Table 2.

Percent agreement reveals the accuracy of the rotation calculation method to be highest from 15° to 55°. In this range there is a 98% probability that the calculated rotation is within 5° of the actual rotation (Table 2). The lowest agreement was found in the 60° to 70° range.

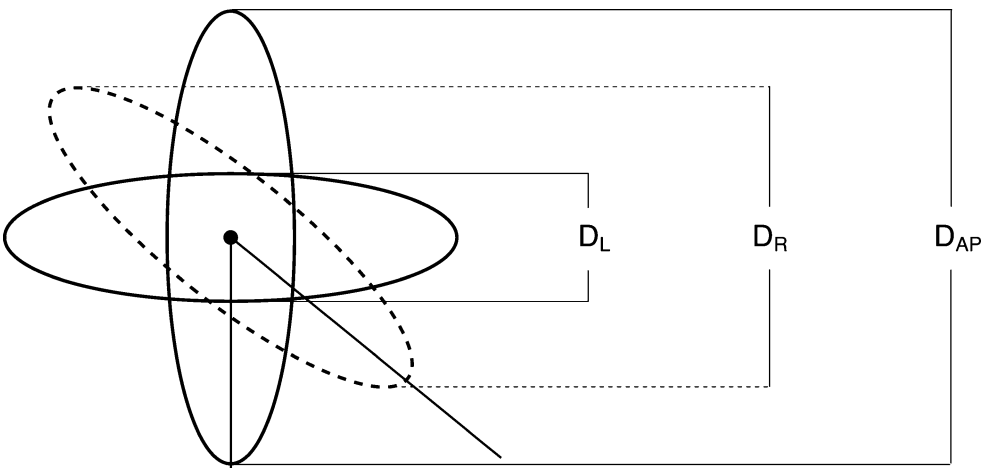

Fig. 7 Ellipse demonstrating major, minor, and rotated dimensions (D_{AP}, D_L, and D_R, respectively)

Table 1 Measurement ratios for given rotation angle values

Ratio	Rotation angle
1.0	0°
0.98	10°
0.94	20°
0.87	30°
0.77	40°
0.64	50°
0.5	60°
0.34	70°
0.17	80°
0.0	90°

ICC (2,1) scores for the model humerus and aluminum phantom, as defined by Altman's criteria, [28] indicate very good reliability of the rotation calculation method (Table 2). The interobserver ICC (2,1) for calculated rotation of the model humerus was 0.9948. The interobserver ICC (2,1) for calculated rotation of the aluminum phantom was 0.9982.

Discussion

Cubitus varus deformity is facilitated by malrotation of the distal fragment in SCHFs. Long-term effects of CVD include disturbance of the humerus's mechanical axis causing lateral collateral ligament stretch producing posterolateral rotatory instability of the elbow joint [26]. This study was designed to test a novel method of measuring SCHF fragment malrotation in order to better assess fracture alignment pre- and postreduction and decrease incidence of CVD.

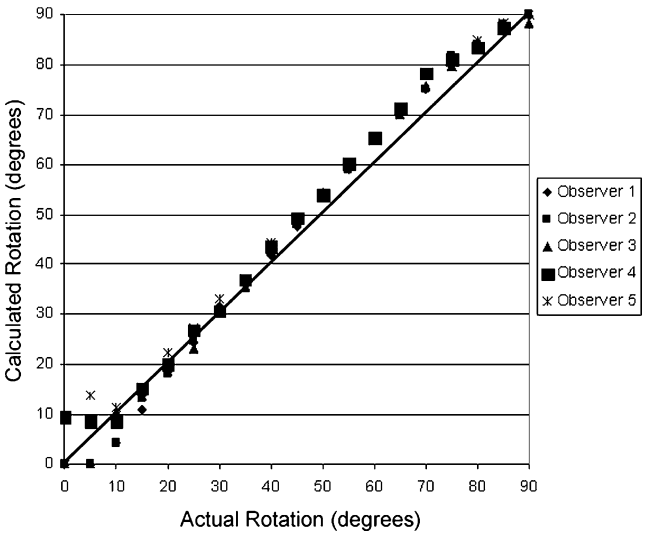

Fig. 8 Calculated rotation versus actual rotation in supracondylar humerus fracture model

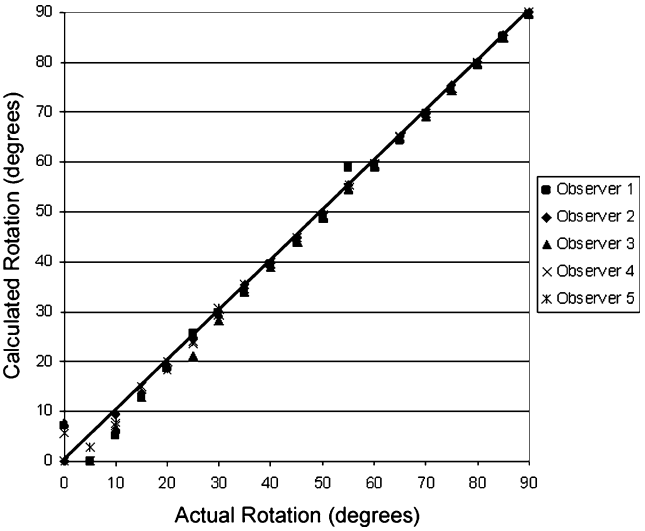

Fig. 9 Calculated rotation versus actual rotation in aluminum phantom model

Agreement and interobserver ICC (2,1) values for this study indicate this method of calculating malrotation is accurate and reliable. This reliability was possibly enhanced by our use of digitized radiographs and the ability to enlarge the images for measurement; however, reliability comparisons of manual and digital radiograph measurements have been shown to be comparable [29].

Accuracy of this method was highest from 15° to 55° with 98% of calculated rotation values within 5° of the actual rotation within this range (Table 2). This is advantageous given that 30°–45° is reported as the maximum allowable rotation and therefore accuracy within this range is most important [27]. The decreased accuracy outside of this range was felt to be of less importance as a reduction in the 0° to 10° range will be obvious to the trained eye, likewise the need for better reduction at rotations of 60° or greater should be readily perceived without specific knowledge of the rotation.

The increased accuracy within the first 55° of rotation was attributed to the greater ease of identifying the fracture

Table 2 Percent agreement within 3°/5° of actual rotation and intraclass correlation coefficient (2,1) for model humerus and aluminum phantom

Rotation interval	Model humerus	Aluminum phantom
0°–10°	47/73	40/80
15°–25°	93/100	93/100
30°–40°	87/100	100/100
45°–55°	20/93	93/100
60°–70	0/53	100/100
75°–90°	55/80	100/100
Net (0°–90°)	51/83	88/97
ICC (2,1)	0.9948	0.9982

lines as the irregular contours of the humerus do not begin to overlap and complicate visualization until approximately 45° of rotation. Greater accuracy within the 55°–90° range, however, could presumably be achieved by using lateral views of the elbow for the proximal and distal measurements, thus making the cortices more easily identifiable in this range. For this calculation a modification of Eq. 3 would be necessary as the relationship of the fragments would be a function of arc sine rather than arc cosine.

The decreased accuracy of this method in the 0° to 10° range was attributed to the nature of the cosine function itself. In this range, only minute changes in the measurements can greatly influence the calculated rotation; this is illustrated in Table 1 by the increasing value of the intervals between the ratios. Similarly the 0° to 10° range is where calculated rotation of the aluminum phantom was least accurate. As mentioned previously this was felt to be of little significance as the shoulder can easily compensate for 10° of fragment rotation and an anatomic reduction should be readily apparent.

Application of this method in the clinical setting requires AP and lateral radiographs of the elbow joint. As stated previously, the distance between the medial-most and lateral-most aspects of the proximal and distal fracture lines should be measured. On the lateral film, the distance between the anterior-most and posterior-most aspects of the distal fragment should be measured (Fig. 6). To perform the calculation, subtract the lateral distance from the proximal AP distance; this is your numerator. Subtract the lateral distance from the distal AP distance; this is your denominator. Divide the numerator by the denominator (see Eq. 4), the quotient should be a number from 0 to 1.0. To calculate the angle of malrotation, perform the arc cosine function on this number. Knowledge of the ratios that correlate to a given angle of rotation allows for accurate approximation if a calculator is not available (Table 1).

Other techniques for quantifying SCHF malrotation are few. Lőnroth described a method in which multiple radiographs are taken at 5° increments about the fracture site [30]. The two radiographs demonstrating the greatest fracture-line dimension of the proximal and distal fragments are identified and the difference between angles at which the radiographs were taken is calculated and is considered the estimated malrotation. Gordon et al. described a method of estimating malrotation that they call the "lateral rotational percentage" [31]. Using a lateral view of the elbow, the lateral rotational percentage is calculated by dividing the absolute displacement of the proximal humeral metaphysis measured at the fracture site by the dimension of the distal humerus at the fracture site. The resulting quotient is multiplied by 100, producing the lateral rotational percentage. Von Laer described a similar calculation called the rotation failure quotient [32]. Computerized tomography (CT) has also been used to determine malrotation [24].

While knowledge of fragment malrotation within 5° is certainly adequate for assessing reduction adequacy, the method of Lőnroth exposes the patient to far more radiation than the method we have described. Gordon and von Laer's methods provide the practitioner with an estimation of the quality of reduction; however, they do not yield a measure in degrees that is easily translated into accepted clinical parameters. While CT is certainly an accurate method of determining malrotation, its cost in comparison to radiographs makes it a less attractive option.

This study has limitations that deserve consideration. First, this method was tested on models and not in the clinical setting. While promising application of this method to models does not guarantee clinical success, we felt that the use of models was justified as accuracy can only be assessed if the rotation of the fracture fragment is known at the time the radiographs are taken. Only simultaneous CT of the fracture site would allow for radiographic accuracy to be measured and such a scenario would be logistically implausible and subject to prohibitive factors such as unnecessary irradiation of the patient.

Fracture comminution is a potentially confounding element that would preclude accurate rotation assessment with this method. As a comminuted fracture would likely be addressed through an open approach allowing direct visualization, we feel this is a moot point. Although we did not apply this method to an obliquely oriented fracture, its accuracy should not be altered if done so.

Poor radiographic technique is a potential source of error with any radiographic measurement. For greatest accuracy using this method, true AP and lateral radiographs are required. Application of this method using a radiograph that is not a true AP view may result in underestimation of the degree of rotation as the distal-measured dimension will be shortened and the proximal-measured dimension may or may not be shortened. If the proximal dimension exceeds the distal dimension then the radiograph is not a true AP and should be repeated. Use of a radiograph that is not a true lateral view will affect the calculated rotation only insomuch as the measurements' scale factor is reduced, thus decreasing its resolution, but accuracy should not be significantly compromised. Differences in radiograph magnification are another potentially confounding factor. Similar to the use of a radiograph that is not a true lateral, a change in scale factor is likely the most significant outcome with little impact on accuracy. Use of identical techniques for the AP and lateral radiographs, however, will obviate this issue. If the calculated rotation following reduction is in doubt or identification of the fracture lines is difficult, CT should be performed for definitive measure-

ment, especially if the rotation is near the limit of acceptability.

Finally, this method cannot differentiate definitively between internal and external rotation at the fracture site. As over 95% of SCHFs are extension type and generally result in internal rotation of the distal fragment [1], it can usually be presumed that malrotation in pre-reduction radiographs is internal. Following reduction, this method can be used to check whether the rotation is within the accepted range and if further correction is indicated; however, the direction of malrotation should be found through physical exam if not readily apparent on radiographs.

CVD is facilitated by malrotation of the distal fragment in SCHFs. Long-term outcomes of CVD demonstrate disturbance of the humerus's mechanical axis causing lateral collateral ligament stretch producing posterolateral rotatory instability of the elbow joint. The present study was designed to test a novel method of measuring SCHF fragment malrotation in order to better assess fracture alignment pre- and postreduction and decrease incidence of CVD. Agreement and interobserver ICC (2,1) values for this study indicate this cost-effective method of calculating malrotation is accurate, reliable, and warrants clinical application.

Acknowledgements The authors wish to thank Debra Sala, MS PT, and Tony Smart, RT, for their help in this investigation. The authors also wish to thank Lippincott Williams and Wilkins for permission to include the photograph of cubitus varus deformity in a pediatric patient (Figure 3A, p 330 from Uchida Y, Ogtata K, Sugioka Y. A new three-dimensional osteotomy for cubitus varus deformity after supracondylar fracture of the humerus in children. *J Ped Orthop* 1991;11:327–331).

References

1. Herring JA. Fractures about the elbow. In: Herring JA, editors. Tachdjian's pediatric orthopaedics. Vol 3. 3rd ed. Philadelphia: W. B. Saunders Company; 2002 p. 2139–217.
2. Kasser JR, Beaty JH. Supracondylar fractures of the distal humerus. In: Kasser JR, Beaty JH, editors. Rockwood and Wilkin's fractures in children. 5th ed. Philadelphia: Lippincott Williams and Wilkins; 2001. p. 577–623.
3. de las Heras J, Duran D, de la Cerda J, Romanillos, et al. Supracondylar fractures of the humerus in children. Clin Orthop 2005;432:57–64.
4. Battaglia TC, Armstrong DG, Schwend RM. Factors affecting forearm compartment pressures in children with supracondylar fractures of the humerus. J Pediatr Orthop 2002;22:431–39.
5. Minkowitz B, Busch MT. Supracondylar humerus fractures: current trends and controversies. Orthop Clin N Am 1994;25:581–94.
6. Mitsunari A, Muneshige H, Ikuta Y. Internal rotation deformity and tardy ulnar nerve palsy after supracondylar humeral fracture. J Shoulder Elbow Surg 1995;4:23–29.
7. Takahara M, Sasaki I, Kimura T, et al. Second fracture of the distal humerus after varus malunion of a supracondylar fracture in children. J Bone Joint Surg (Br) 1998;80B:791–97.
8. Wilkins KE. The operative management of supracondylar fractures. Orthop Clin N Am 1990;21:269–89.
9. Bellemore MC, Barrett IR, Middleton RWD, et al. Supracondylar osteotomy of the humerus for correction of cubitus varus. J Bone Joint Surg (Br) 1984;66B:566–72.
10. Canale T. Fractures and dislocations in children. In: Canale T, editor. Campbell's operative orthopaedics. Vol 2. 10th ed. Philadelphia: Mosby; 2003. p. 1391–565.
11. Davis RT, Gorczyca JT, Pugh K. Supracondylar humerus fractures in children. Clin Orthop 2000;376:49–55.
12. Price CT, Phillips JH, Devito DP. Management of fractures. In: Morrisey RT, Weinstein SL, editors. Lowell and Winter's pediatric orthopaedics. Vol 2. 5th ed. Philadelphia: Lippincott Williams and Wilkins; 2001. p. 1319–422.
13. Wilkins KE. Changing patterns in the management of fractures in children. Clin Orthop 1991;264:136.
14. Amspacher JC, Messenbaugh JFJ. Supracondylar osteotomy of the humerus for correction of rotational and angular deformities of the elbow. South Med J 1964;57:846–50.
15. Badhe N, Howard P. Olecranon screw traction for displaced supracondylar fractures of the humerus in children. Injury 1998;29:457–60.
16. Mitchell WJ, Adams JP. Supracondylar fractures of the humerus in children: a ten-year review. JAMA 1961;175:573–77.
17. Nacht JL, Ecker ML, Chung SMK, et al. Supracondylar fractures of the humerus in children treated by closed reduction and percutaneous pinning. Clin Orthop 1983;177:203–09.
18. Smith L. Deformity following supracondylar fractures of the humerus. J Bone Joint Surg (Am) 1960;42A:235.
19. Vahvanen V, Aalto K. Supracondylar fractures of the humerus in children. A long-term follow-up study of 107 cases. Acta Orthop Scand 1978;49:225–33.
20. Weiland AJ, Meyer S, Tolo VT. Surgical treatment of displaced supracondylar fractures of the humerus in children. Analysis of fifty-two cases followed for five to fifteen years. J Bone Joint Surg (Am) 1978;56:657–61.
21. Wilkins KE. Supracondylar fractures: what's new? J Pediatr Orthop B 1997;6:110.
22. Arnold JA, Nasca RJ, Nelson CL. Supracondylar fractures of the humerus: the role of dynamic factors in prevention of deformity. J Bone Joint Surg (Am) 1977;59A:589–95.
23. French PR. Varus deformity of the elbow following supracondylar fractures of the humerus in children. Lancet 1959;ii:439–41.
24. Resch H, Helweg G. Significance of rotation errors in supracondylar humeral fractures in the child. Aktuelle Traumatol 1987;17:65.
25. Wilkins KE. Residuals of elbow trauma in children. Orthop Clin N Am 1990;21:291.
26. O'Driscoll SW, Spinner RJ, McKee MD, et al. Tardy posterolateral rotatory instability of the elbow due to cubitus varus. J Bone Joint Surg (Am) 2001;83A:1358–67.
27. Shrout PE, Fleiss JL. Intraclass correlations: uses in assessing rater reliability. Psychol Bull 1979;86:420–28.
28. Altman DG. Practical statistics for medical research. 1st ed. New York, NY: Chapman and Hall; 1991.
29. Specogna AV, Birmingham TB, DaSilva JJ, et al. Reliability of lower limb frontal plane alignment measurements using plain radiographs and digitalized images. J Knee Surg 2004;17:203–10.
30. Lőnroth H. Measurement of rotational displacement in supracondylar fractures of the humerus. Acta Radiol 1962;57:65–70.
31. Gordon JE, Patton CM, Luhmann SJ, et al. Fracture stability after pinning of displaced supracondylar distal humerus fractures in children. J Pediatr Orthop 2001;21:313–18.
32. von Laer L. Die supracondyläre humerusfraktur im Kindesalter. Arch Orthop Trauma Surg 1979;95:123–40.